

ROBUST SCALABLE VEHICLE CONTROL VIA NON-DIMENSIONAL VEHICLE DYNAMICS

S. Brennan & A. Alleyne
Dept. of Mechanical & Industrial Engineering
University of Illinois at Urbana-Champaign
1206 W. Green Street
Urbana, IL 61801

ABSTRACT

A temporal and spatial re-parameterization of the well-known linear vehicle Bicycle Model is presented. This parameterization utilizes non-dimensional ratios of vehicle parameters called pi-groups. Investigation of these pi-groups using compiled data from 44 published sets of Vehicle Dynamics reveals that the data does not span the pi-space, but instead follows a multi-dimensional line through pi-space with a Gaussian distribution about this line. This Gaussian distribution suggests numerical values for an ‘average’ vehicle as well a maximum perturbation about the average. Stability analysis in the pi-space is then considered. A state-feedback controller is designed that utilizes the pi-space curve and the expected pi-perturbations to robustly stabilize the class of all vehicles subject to the distribution of vehicle parameters observed in the literature. Experimental verification is obtained using a scaled vehicle.

I. Motivation

The field of Robust Control made large advances in the 1980’s and a framework for formally dealing with system uncertainty is fairly well understood (Zhou and others 1996). However, in most of the approaches to Robust Control, there has been little work done to utilize a specific non-dimensional structure to the problem in order to define plant deviations. An example of a system where a specific structure could be exploited is that of vehicle control. With extensive previous work that has been done on Automated Highway systems or Intelligent Vehicles (Shladover 1995), it has been found that repeated manipulation of the various controllers is necessary to achieve adequate performance for different vehicles. This re-calibration of vehicle controllers is expected since the actual vehicle plant is changing from vehicle-to-vehicle. In this work we consider ways to design a controller that is robust to these variations and is based on perturbations of a system plant around some ‘average’ vehicle. Previous work (Brennan 1999) has indicated that it is difficult to predict the variation magnitudes in the system dynamics before a new vehicle is built. An additional but related problem is that the notion of an ‘average’ vehicle is unclear. Average parameters are highly desirable in controlled vehicles to ensure appropriate controller development, but a methodology to compare systems based on their physical parameter dimensions has

not yet been formalized in the field of control. The goal of this paper is therefore two-fold: first, to develop a numerically appropriate framework that allows parameter-based comparisons between vehicles, and second to obtain a controller that is robust to vehicle-to-vehicle parameter variation.

What the control architecture often overlooks is the fact that single physical parameters do not usually change on a system independent of other parameters. For instance, if the mass of a vehicle is increased, the moment of inertia will increase as well. Although significant control theory has been developed to describe the *dynamic* relationships of a dynamical class of systems, this theory usually doesn’t incorporate *parametric* trends introduced by the physical design of similar systems. In vehicle systems for instance, this paper shows later that parameter interdependence can be described quite well by a line through parameter space.

In control theory, plant variations or uncertainty are usually resolved using two methods: robust control or adaptive control. Robust control seeks to design a controller unresponsive to variations, while adaptive control seeks to identify the model parameters and include the identified variations into the control of the plant. Examples of adaptive approaches applied to vehicle control include neural networks to identify and adapt to road friction changes (Shiotsuka and others 1993). Robust control to address road friction variation and velocity variation are presented in (Tagawa and others 1996), and road-friction uncertainty robustness is presented in (Ono and others 1994). Naturally, mixed approaches can be implemented; for instance in (Horiuchi and others 1996), where adaptive control is used to identify the vehicle model and robust control is used to stabilize the vehicle in the presence of expected model perturbations and disturbances. In the context of this research, the focus will be on categorizing the uncertainty within a non-dimensional framework. Therefore, the robust approach will be the tool used to consider model variability.

A method to incorporate model variability was suggested by first answering the question: what is the best method to compare systems of different parameter dimensions but that are likely described by the same dynamics? This problem was examined in (Brennan 1999) when attempting to compare published work between several authors that have used differing vehicles. A similar problem was first addressed by Freude in 1850’s in the study of ship design, and formalized solution was obtained

with the Buckingham Pi Theorem (Buckingham 1914) in the early 1900's. This theorem determines the minimum number of parameters, grouped into non-dimensional ratios, needed to span the parameter space over which dynamics are expected to operate. The well-known Reynolds number, Freude number, and Nusselt numbers are just a few of the parameters identified for fluid/thermal systems using this method.

The outline of the paper is as follows. Section II introduces the linear, planar vehicle model and the non-dimensional counterpart. Additionally, the concept of non-dimensional comparisons are introduced. Section III then presents distributions of the non-dimensional parameters for vehicles found in the literature and thus defines numerically an 'average' vehicle. To relate the use of the non-dimensional parameters to common Vehicle Dynamics, Section IV develops a classical expression for vehicle stability and shows how this criterion is simplified further using inferred non-dimensional relationships. Section V uses the distributions of Section III and develops a feedback controller robust to vehicle-to-vehicle variation. Furthermore, a sample implementation on a scaled test vehicle is provided. A Conclusions section summarizes the main points of the paper.

II. Vehicle Dynamics and Pi Analysis

The vehicle model considered in this paper describes the planar vehicle dynamics when front wheel steering inputs are applied. For brevity, rear wheel steering inputs and torque inputs are not considered in this paper, but the following analysis is easily extended to these cases. The vehicle model is assumed to be linear, and described by the well-known bicycle model (Alleyne 1997; Wong 1993) as follows:

$$\begin{aligned} \frac{dx}{dt} &= Ax + Bu & x &= \begin{bmatrix} y & \frac{dy}{dt} & \theta & \frac{d\theta}{dt} \end{bmatrix}^T \\ y &= Cx + Du \end{aligned} \quad (1)$$

with

$$A = \begin{bmatrix} 0 & 1 & 0 & 0 \\ 0 & -\frac{C_{af} + C_{ar}}{mV} & \frac{C_{af} + C_{ar}}{m} & \frac{b \cdot C_{ar} - a \cdot C_{af}}{mV} \\ 0 & 0 & 0 & 1 \\ 0 & \frac{b \cdot C_{ar} - a \cdot C_{af}}{I_z \cdot V} & \frac{a \cdot C_{af} - b \cdot C_{ar}}{I_z} & -\frac{a^2 \cdot C_{af} + b^2 \cdot C_{ar}}{I_z \cdot V} \end{bmatrix}$$

$$B = \begin{bmatrix} 0 & \frac{C_{af}}{m} & 0 & \frac{a \cdot C_{af}}{I_z} \end{bmatrix}^T$$

For a Classical Controls perspective, the corresponding transfer function from front steering input to yaw rate can be written as:

$$\frac{\dot{\Psi}(s)}{d_f(s)} = \frac{\frac{C_{af} a}{I_z} \cdot s + \frac{C_{af} C_{ar} L}{m I_z V}}{D(s)} \quad (2)$$

where the characteristic polynomial is:

$$D(s) = s^2 + \left(\frac{C_{af} + C_{ar}}{mV} + \frac{C_{af} a^2 + C_{ar} b^2}{I_z V} \right) \cdot s + \frac{C_{af} C_{ar} L^2}{m I_z V} - \frac{(a C_{af} - b C_{ar})}{I_z}$$

The vehicle parameters are defined as follows for a scaled Illinois Roadway Simulator (IRS) (Brennan 1999; Brennan and Alleyne 1999) vehicle used in the experimental results of Section V.

- m = vehicle mass, kg (6.02),
- I_z = vehicle moment of inertia, kg-m² (0.153),
- V = vehicle lateral velocity, m/s (1.98)
- a = distance from C.G. to front axle, m (0.137)
- b = distance from C.G. to rear axle, m (0.222)
- L = vehicle length, $a + b$, m (0.359)
- C_{af} = front cornering stiffness (2 tires), N/rad (40)
- C_{ar} = rear cornering stiffness (2 tires), N/rad (52)

The values in parentheses are the numerical values for a typical scale vehicle used in confirmatory testing of the controller later in this paper. These parameters can be grouped into the following non-dimensional units if all length coordinates are normalized using the vehicle length, and all time coordinates are normalized by the length of time a vehicle needs to travel its own length at a velocity V , or L/V .

$$D_1 = \frac{a}{L}, \quad D_2 = \frac{b}{L}, \quad D_3 = \frac{C_{af} L}{mV^2}, \quad D_4 = \frac{C_{ar} L}{mV^2}, \quad D_5 = \frac{I_z}{mL^2} \quad (3)$$

Noting that the Laplace variable 's' and the yaw rate measurement have units of [sec⁻¹]; both can be normalized to s^* and $\dot{\Psi}^*$ by factoring the term (V/L) . The input is an angle and is therefore already a non-dimensional term. After substituting the Pi parameters, the Classical Control transfer function of Equation (2) can be rewritten as:

$$\frac{\dot{\Psi}^*}{d_f^*} = \frac{\frac{\Pi_1 \Pi_3}{\Pi_5} \left(s^* + \frac{\Pi_4}{\Pi_1} \right)}{s^{*2} + \left(\Pi_3 + \Pi_4 + \frac{\Pi_1^2 \Pi_3 + \Pi_2^2 \Pi_4}{\Pi_5} \right) s^* + \frac{\Pi_3 \Pi_4}{\Pi_5} - \frac{\Pi_1 \Pi_3 - \Pi_2 \Pi_4}{\Pi_5}} \quad (4)$$

The state-space form presented previously can also be normalized as follows:

$$x = M \cdot x^* \quad \text{and} \quad \frac{dx}{dt} = \frac{d(M \cdot x^*)}{dt} = \frac{V}{L} \cdot M \cdot \frac{dx^*}{dt}$$

Therefore, Equation (1) can be rewritten as:

$$\begin{aligned} \frac{dx^*}{dt^*} &= \frac{L}{V} M^{-1} A M \cdot x^* + \frac{L}{V} M^{-1} B \cdot u^* = A^* x^* + B^* u^* \\ y^* &= M^{-1} C M \cdot x^* \end{aligned} \quad (5)$$

with $M = \text{diag} \left[L \quad V \quad 1 \quad \frac{V}{L} \right]$

Equation (5) is simply a dimensional time-scaling combined with a coordinate transformation. The A^* and B^* matrices can be rewritten in Pi-form as:

$$A = \begin{bmatrix} 0 & 1 & 0 & 0 \\ 0 & -\Pi_3 - \Pi_4 & \Pi_3 + \Pi_4 & \Pi_2 \Pi_4 - \Pi_1 \Pi_3 \\ 0 & 0 & 0 & 1 \\ 0 & \frac{\Pi_2 \Pi_4 - \Pi_1 \Pi_3}{\Pi_5} & \frac{\Pi_1 \Pi_3 - \Pi_2 \Pi_4}{\Pi_5} & -\frac{\Pi_1^2 \Pi_3 + \Pi_2^2 \Pi_4}{\Pi_5} \end{bmatrix}$$

$$B = \begin{bmatrix} 0 & \Pi_3 & 0 & \frac{\Pi_1 \Pi_3}{\Pi_5} \end{bmatrix}^T \quad (6)$$

Pi-analysis was originally developed to achieve dynamic matching between systems. When the pi-parameters are the same for two systems with differing dimensional parameters, but the same dynamical equations of motion, the systems are said to be *dynamically similar*. Examination of the non-dimensional characteristic equation reveals that if the pi-parameters match between two systems governed by the bicycle model, then the systems will have identical dynamics. Therefore, two systems are dynamically ‘close’ if their numerical values for the pi-parameters are all ‘close’ in the pi-space.

To demonstrate that controller design using the non-dimensional coordinates is straightforward, consider classical pole-placement on a full-sized vehicle. The following published (Alleyne 1997) vehicle parameters were used: $m = 1670$ kg, $I_z = 2100$ kg-m², $a = 0.99$ m, $b = 1.7$ m, $C_{of} = 123,190$ N/rad, $C_{or} = 104,190$ N/rad, and $V = 15$ m/s. The goal of this simple lateral positioning controller is to place the closed-loop poles at $[-10, -15, -20, -25]$ [rad/sec] in the s-space, corresponding to $[-1.79, -2.69, -3.59, -4.48]$ [unitless] in normalized-s space. The gain obtained from performing non-dimensional pole placement is K^* , defined by the following relationship:

$$u^* = K^* \cdot x^* = u = K \cdot x = K(M \cdot x) \Rightarrow K^* = K \cdot M \quad (7)$$

The gain matrix obtained using traditional controller pole-placement is: $K = [7.62, 0.712, 5.70, -0.0856]$. The gain obtained by performing non-dimensional pole-placement is: $[20.5, 10.68, 5.70, -0.478]$. Using the conversion in Equation (7), the non-dimensional gain-matrix predicts that the dimensional gain matrix should be $K = [7.62, 0.712, 5.70, -0.0856]$, exactly as predicted. It should therefore be clear that whether the controller design is conducted in non-dimensional space or in classical dimensional space, the resulting gains are equivalent as long as the gains account for dimensional and temporal conversions.

There are key advantages to designing a vehicle controller in the pi-space versus dimensional space. For a given vehicle, the mass, moment of inertia, and length parameters are approximately constant but the velocity and cornering stiffness change significantly with driving conditions. Thus, all of the pi-parameters are, in general,

time invariant, except for Π_3 and Π_4 . It is well known that the vehicle dynamics change significantly with both velocity and cornering stiffness. Later in this paper it is shown that for a given vehicle, Π_4 is usually some fixed ratio of Π_3 . Therefore, both velocity AND cornering stiffness variations correspond to variations in a single parameter: Π_3 . This is seen Figure 1 where the roots of the Characteristic Polynomial of Equations (2) and (4) are shown with respect to the two different parameters: velocity (represented by ‘o’) and cornering stiffness (represented by ‘x’). On the left is the classical vehicle representation, and on the right the non-dimensional representation. For the variation of the system roots with respect to cornering stiffness, the ratio of front to rear cornering stiffness was assumed to remain the same.

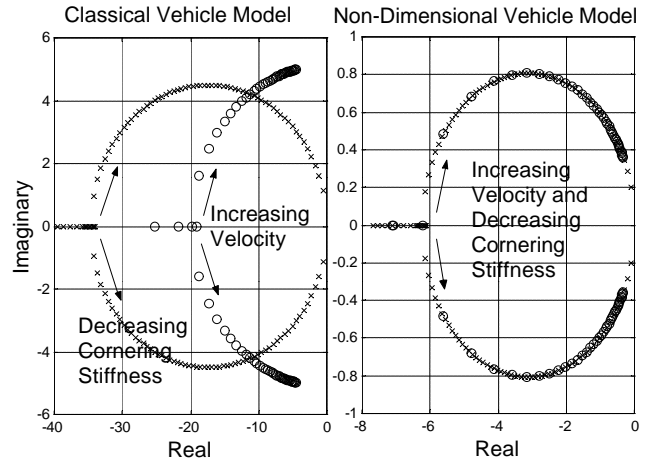


Figure 1. Parameter root loci.

These plots, similar to a Root Locus for controller design, hint that the effect of road-friction variations on the underlying vehicle dynamics is somehow dual to the effect of velocity variations. Therefore, the traditional approach of separately considering these two system parameter variations may possibly be streamlined and combined.

III. Trends in Published Pi Parameters

Section II demonstrates the possible utility of considering the vehicle dynamics in a non-dimensional setting. To determine the expected dynamic variability between vehicles, a distribution of pi parameters was obtained by substituting published vehicle parameters from 44 different vehicles found in the literature. All vehicles were production passenger vehicles. A velocity of 14.6 m/s was used for these calculations, but any velocity could be used: changing velocity simply re-scales the x-axis on the Π_3 and Π_4 plots. Note that the Π_2 parameter is omitted because this parameter is constrained physically by the Π_1 parameter with the physical relationship $\Pi_1 + \Pi_2 = 1$. Figure 2 shows the resulting distributions. In addition, Figure 2 indicates the values of the pi parameters for a

scaled vehicle (Brennan and Alleyne 1999) that will be used in Section V to obtain experimental results.

Clearly, distinct distributions are present for each of the pi-parameters. Considering that the practice of vehicle design is an iterative and evolutionary process, vehicle parameters are expected to eventually cluster toward ‘ideal’ parameters that best satisfy marketing, construction, and driver constraints. An observed statistical distribution suggests to a vehicle designer a particular vehicle ‘norm’. Although the engineering reasons driving this trend are not under discussion here, it is likely that vehicles with parameters far from the mean may represent an of anomalous vehicle. For instance, plotting the pi parameters for a grand-prix vehicle with the passenger vehicles in Figure 2 would require a several-fold increase of the x-axis.

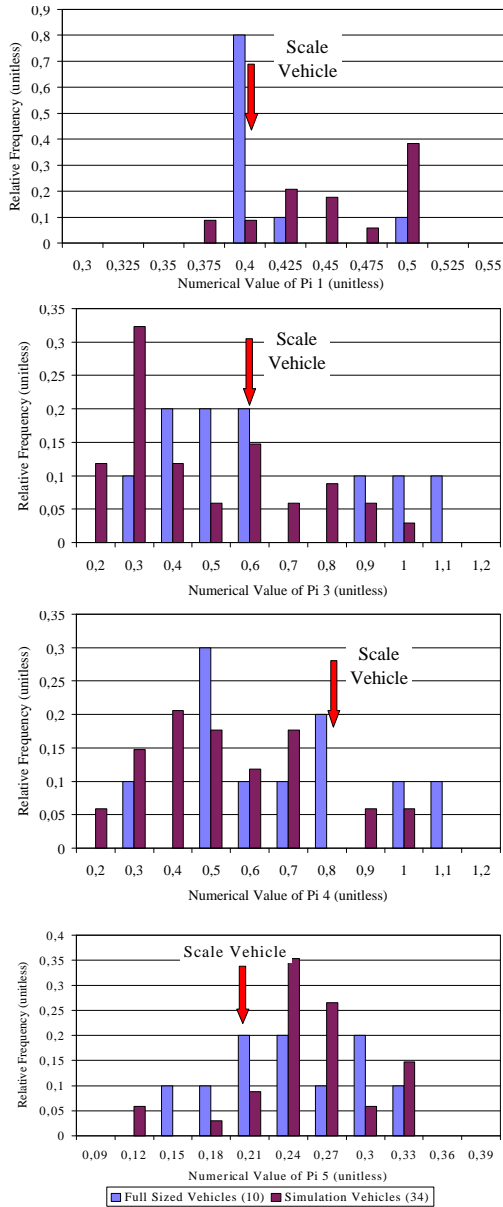


Figure 2. Pi-group distribution.

In addition to providing clues toward vehicle design, the pi distributions provide key information for subsequent controller design. An ‘average’ passenger vehicle would likely have parameters located at the peaks of these distributions. All vehicles appear to lie about this average with some standard deviation in each parameter. Intuitively then, the controller problem of stabilizing any passenger vehicles now becomes a much simpler task of designing a controller to stabilize the above ‘average’ vehicle in the presence of non-dimensional parameter perturbations with the same magnitude as the ‘spread’ seen in the Figure 2 distributions.

IV. Vehicle Stability Analysis

Using the Routh Stability Criterion, the classical yaw-rate stability limits of the open-loop system are easily found. The Routh criterion guarantees stability for Equation (4) if the coefficients of the characteristic equation are all greater than zero. Noting that the Pi values are always positive for vehicles due to physical constraints, stability limits can therefore be found by setting the last term in the denominator equal to zero. The following constraint then guarantees yaw-rate vehicle stability for the linear bicycle model.

$$P_3 P_4 - P_1 P_3 + P_2 P_4 > 0 \quad (8)$$

Back substitution of the pi-values yields:

$$\frac{C_{af} L}{mV^2} \frac{C_{ar} L}{mV^2} - \frac{a}{L} \frac{C_{af} L}{mV^2} + \frac{b}{L} \frac{C_{ar} L}{mV^2} > 0 \quad (9)$$

or

$$\frac{C_{af} C_{ar} L^2}{m(aC_{af} - bC_{ar})} > V_{crit}^2 \quad (10)$$

This is simply the classical expression for the well-known critical velocity above which an oversteer vehicle becomes unstable.

Examination of the Pi inequality in Equation (8) reveals that from a design standpoint the easiest way to improve stability is to increase Π_4 (note that Π_2 cannot be changed independent of Π_1). This parameter represents the relative magnitude of the rear cornering stiffness of the vehicle. The inequality therefore suggests that rear tire adhesion should not be compromised, as is well known for preventing vehicle oversteer instability (Wong 1993).

The previous stability criterion can be simplified by considering the information inherent in the parameter distributions. Knowing that $\Pi_2 = 1 - \Pi_1$ due to physical constraints, a relationship is sought between Π_3 and Π_4 (the non-dimensional cornering stiffness parameters) that simplifies the stability constraint of Equation (8); Π_3 is plotted versus Π_4 in Figure 3.

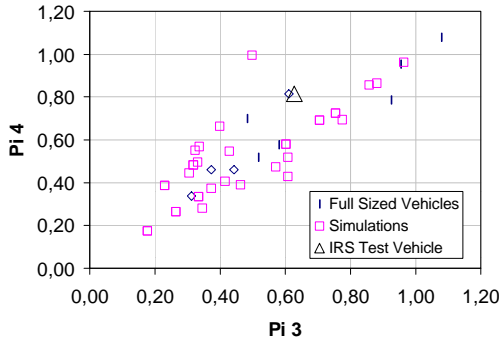


Figure 3. Relationship between Pi3 and Pi4.

A general relationship was found to exist where $\Pi_3 \cong \Pi_4$. Noting the physical meaning of these parameters, this indicates the rear cornering stiffness is about the same as the front to a first approximation. This is intuitive because both tires are made from the same material and are driving on the same road surface. However, this data must be taken with some question before accepting this relationship as fact since front & rear tire characteristics can vary on a vehicle. Assuming that the front and rear cornering stiffness are equal as a first approximation, the constraint on vehicle stability can now be reduced to the expression:

$$\frac{P_3 + 1}{2} > P_1 \quad (11)$$

Which is simply a line dividing the Π_1 vs. Π_3 space. A plot of experimental values of Π_1 versus Π_3 is shown in Figure 4 with the above stability line included.

From the inequality in Equation (11), it can be inferred that the vehicles farthest away from this line would likely be most stable. To test this idea, the pole locations of the closest and farthest vehicles are shown in Figure 4. It was confirmed that the vehicle with the most stable pole locations was the vehicle farthest away from the above line. The least stable vehicle, with pole locations closest to the imaginary axis in the s-plane, was in fact the vehicle closest to the above stability line.

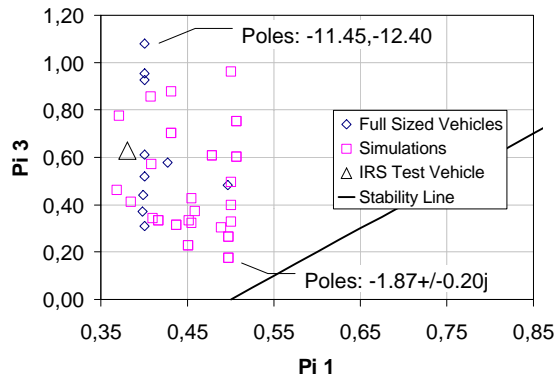


Figure 4. The stability line in the pi space.

The previous Pi analysis has revealed a general *linear* design criterion that may be used in the construction of a

vehicle to estimate open-loop stability. This approach demonstrates that accounting for parameter inter-relationships can greatly simplify stability analysis. Moreover, this can quickly and easily be done over a range of different vehicle sizes and vehicle parameters. The same concept is now considered for specific use in controller design.

V. Robust Controller Design

The assumption in the following controller design is that the distributions representing vehicle-to-vehicle variations should serve as the robustness measure of the controller. A first approach to classify the system uncertainty would be to note the possible variation in each pi-parameter, and then obtain some uncertainty bound that spans all possible permutations of the five pi-parameters, thus creating a hyper-cube in parameter space. A problem with this approach is that it ignores parameter interdependence. Figure 3 shows that most experimental vehicles would only exist in a small subset of such a space. In the simplest case, the parameters would span the parameter-space as a line. Thus, measurement of one parameter would allow the prediction of all other parameters. This will never happen with physical systems due to true plant-to-plant variations and measurement error. Thus, a Gaussian distribution of experimental data about a line through parameter space would be the reasonable assumption for a relationship. As will be shown in this section, this is in fact the case for vehicle dynamics based on the obtained vehicle distributions.

Although the non-dimensional system matrices in Equation (6) are composed of nonlinear pi-parameter functions, these functions can be approximated by using experimental data to determine the best-fit line via simple regression. Additional perturbations are then added to each line such that all experimental data are included in the perturbation sector. Thus, a realistic parameter bound is obtained for the vehicle system. Π_3 is chosen as the independent variable because this variable has the most variation due to velocity and cornering stiffness changes. Note that Π_4 undergoes the same variations, but as was shown previously Π_4 can be represented as a linear function of Π_3 .

Each pi-function in the non-dimensional matrices of Equation (6) is written as a function of Π_3 and some perturbation. This function is approximated as a line with slope m and intercept b , and a perturbation is included in each function to span the error. The state space system matrices can be rewritten as:

$$A = \begin{bmatrix} 0 & 1 & 0 & 0 \\ 0 & -\Pi_3 - f_1 & \Pi_3 + f_1 & f_2 \\ 0 & 0 & 0 & 1 \\ 0 & f_4 - f_3 & f_3 - f_4 & f_5 \end{bmatrix} \quad B = \begin{bmatrix} 0 & \Pi_3 & 0 & f_3 \end{bmatrix}^T \quad (12)$$

where

$$P_3 \in [0.17, 1.2]$$

$$f_1(\Pi_3, \Delta_1) = \Pi_4 \approx m_1 \cdot \Pi_3 + b_1 + \Delta_1$$

$$f_2(\Pi_3, \Delta_2) = \Pi_2 \Pi_4 - \Pi_1 \Pi_3 \approx m_2 \cdot \Pi_3 + b_2 + \Delta_2$$

$$f_3(\Pi_3, \Delta_3) = \Pi_1 \Pi_3 / \Pi_5 \approx m_3 \cdot \Pi_3 + b_3 + \Delta_3$$

$$f_4(\Pi_3, \Delta_4) = \Pi_2 \Pi_4 / \Pi_5 \approx m_4 \cdot \Pi_3 + b_4 + \Delta_4$$

$$f_5(\Pi_3, \Delta_5) = -\left(\Pi_1^2 \Pi_3 + \Pi_2^2 \Pi_4\right) / \Pi_5 \approx m_5 \cdot \Pi_3 + b_5 + \Delta_5$$

An example of the linear regression fit of function f_5 is shown in Figure 5. A normal probability plot of the residuals of the regression fit is shown in Figure 6, where clear normality trends are demonstrated by the fact that the residuals are well-approximated by a line connecting the 25 and 75 percentiles, and zero bias is demonstrated by the fact the line passes through the point (0,50%).

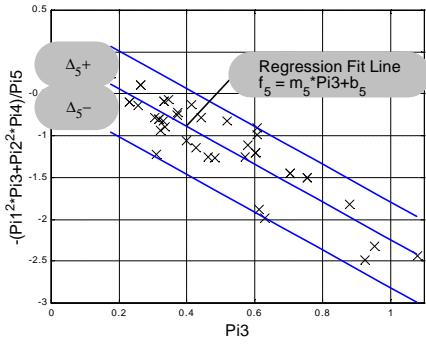


Figure 5. Example parameter fit of function f_5 .

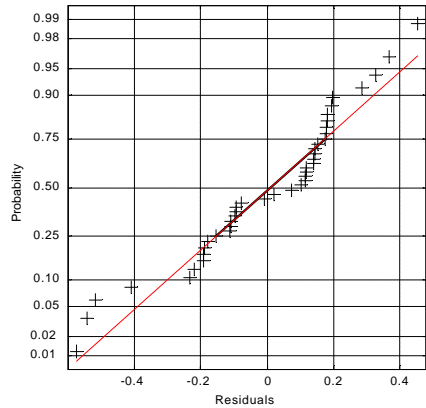


Figure 6. Normal probability plot of residuals.

| f_i | Slope m_i | Intercept b_i | Δ_i Min | Δ_i Max |
|---------|----------------|--------------------|-------------------|-------------------|
| Π_3 | 1.000 | 0.000 | N/A | N/A |
| 1 | 0.818 | 0.130 | -0.198 | 0.209 |
| 2 | 0.069 | 0.048 | -0.155 | 0.156 |
| 3 | 2.005 | -0.091 | -0.311 | 0.365 |
| 4 | 2.398 | 0.059 | -0.726 | 0.891 |
| 5 | -2.262 | 0.019 | -0.574 | 0.453 |

Table1. Parameter regression results for each function f_i .

Note that the system matrices A and B from equation (6) now have a linear dependence on Π_3 and perturbation terms. That is, both matrices can be written as a linear polynomial dependent on Π_3 and the perturbation terms. For instance, the nondimensional matrix A can be rewritten as:

$$A(\Pi_3, \Delta_1, \Delta_2, \dots) = A_0 + A_1 \cdot \Delta_1 + A_2 \cdot \Delta_2 \dots + A_n \cdot \Delta_n \quad (13)$$

The matrix B can be rewritten in a similar manner. By substitution of each function, f_i , from Table 1 into the nondimensional matrices of Equation (6), the numerical values of each A_i in Equation (13) can be found to form nondimensional A and B matrices with linear parameter dependence on Π_3 and perturbations. A system form with this linear parameter dependence allows the use of commercial convex LMI optimization routines to design the control law (Gahinet and others 1995). In this work, the optimization returns a fixed-gain, state feedback controller.

Obtaining a single fixed gain controller that stabilizes the vehicle model given in Equation (1) over a wide range of velocities and road surface conditions is quite challenging (Guldner and others 1996). Quite often, a reasonable approach is to schedule the controller with respect to speed or road condition, if that can be known. If a very large range of parameter perturbations is to be considered, it is quite possible that the LMI optimization approach will fail to reach a solution because one will not exist. For the sake of computational feasibility, a stabilizing controller was sought that stabilized the given class of vehicles about a particular Π_3 value in the presence of Π_3 perturbations. In addition, closed loop pole-placement constraints were imposed on the system. To obtain valid non-dimensional pole-placement regions, it should be noted that the non-dimensional system will always have the same phase angle as the dimensional system. This is because the mapping of the pole locations from one domain to another requires only a temporal modification, which corresponds only to changing the scale of the s-plane axes. To define the closed loop responses via pole placement, we first impose damping constraints on the system: i.e. the non-dimensional poles were made to lie in a cone in the left-half s-plane with vertex on the origin and a vertex angle of $\tan^{-1}(3\pi/4)$ rad or ~ 67 degrees. This corresponds to a minimum damping ratio of 0.39, and a maximum step response overshoot of 26.4%. In addition, the poles were sector bounded to be in the region $-7 < s^* < -1$, in order to impose some limit on the rise-time and system bandwidth.

To demonstrate the variability in the vehicle dynamics due to changing parameters, the pole locations of the open-loop system corresponding to the Bicycle Model are shown in Figure 7. These pole locations correspond to the vertex points of the perturbation hypercube in parameter space.

To show the similar structure between the two spaces, both the non-dimensional and standard pole-plots are shown.

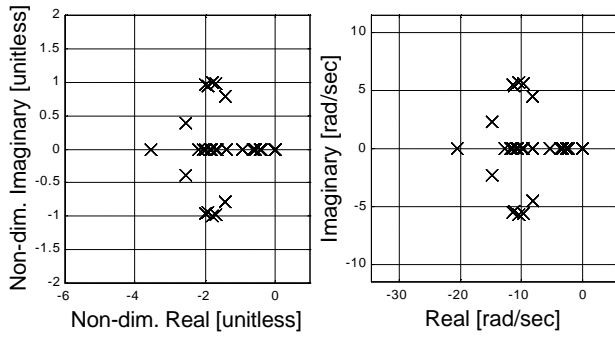


Figure 7. The vertex open-loop pole locations.

The MATLAB LMI Toolbox (Gahinet and others 1995) was used to design a controller to meet the pole-placement specifications about a fixed Π_3 value of 0.63 with Π_3 perturbations allowable up to 0.03, and all other perturbations ranging over the values in Table 1. This controller should therefore stabilize any vehicle with Π_3 values between 0.6 and 0.65 that is described by the distributions of Figure 2. The Π_3 value corresponds to an average, full-size vehicle driving at a speed of 15 m/s (35 mph), and a corresponding scale vehicle (Brennan and Alleyne 1999) speed of 1.95 m/s. The non-dimensional gain matrix was found to be:

$$K^* = [8.1908 \quad 6.3391 \quad 7.7336 \quad 0.5499] \quad (14)$$

Using the vertex points of the perturbation hyper-cube, the closed-loop pole locations were determined in both dimensional and non-dimensional pole space. The resulting pole locations are shown in Figure 8.

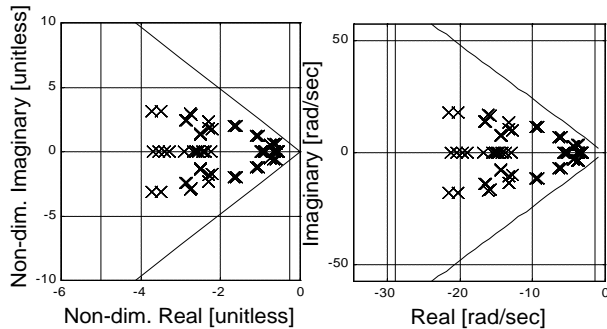


Figure 8. The vertex closed-loop pole locations.

The associated time-domain simulation plots of lateral position and yaw rate are shown in Figure 9 for a series of closed loop vehicle lateral step responses. These responses correspond to a 1.3 m step-change in lateral position. Here, each step response corresponds to a vehicle representing one of the perturbation combinations providing the pole locations show in Figures 7 and 8. The closed loop dynamics of these vehicles have characteristics

corresponding to a single fixed gain feedback operating at each vertex of a pi-perturbation hyper-cube.

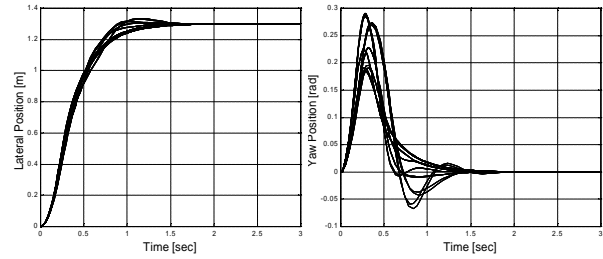


Figure 9. Robust lateral position and yaw-responses.

To test the controller on an experimental vehicle, the Illinois Roadway Simulator (IRS) was utilized. The IRS is a scaled vehicle testbed for Vehicle Dynamics and Controls (Brennan and Alleyne 1999). It has been shown previously that the IRS vehicles do contain a high degree of dynamic similitude with actual full size vehicles as illustrated in Figure 2. A picture of an IRS scale vehicle is given in Figure 10 and a detailed description can be found in (Brennan and Alleyne 1999).

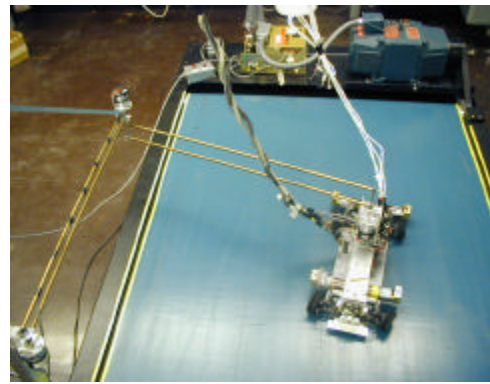


Figure 10. IRS and scaled vehicle.

For this scaled vehicle, a controller gain was obtained using the transformation of Equation (7). The resulting gain, after substitution of the vehicle parameter values with length $L = 0.359$ m and velocity 1.95 m/s, is shown below for the scale vehicle

$$K = [22.85 \quad 3.2508 \quad 7.7336 \quad 0.1011] \quad (15)$$

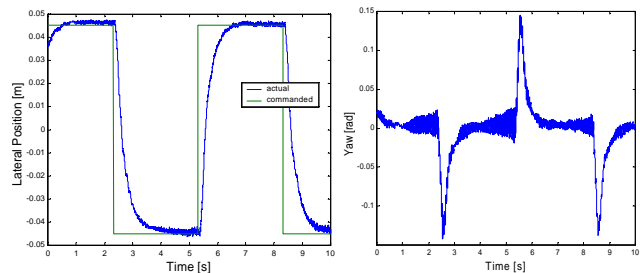


Figure 11. Closed loop lateral pos. and yaw responses.

Experimental lateral position and yaw-rate responses were then obtained, as shown in Figure 11. As can be seen in the figures, both the lateral position and yaw angle responses

were within the bounds as predicted by the CL pole locations and as predicted by the simulation step responses.

The controller could be redesigned for different values of Π_3 and different distributions. However, as mentioned earlier, under large variations in Π_3 a solution to the optimization problem may not be guaranteed. Since Π_3 varies primarily with cornering stiffness and vehicle speed, it may be possible to schedule robust controller designs with respect to vehicle velocity that can be readily measured. The robust controller would then be primarily required to incorporate and accommodate vehicle-to-vehicle structural variations in cornering stiffness. Thus, this controller approach may be quite useful as an initial controller methodology for stabilizing a new and unidentified vehicle.

Conclusions

The temporal and spatial re-parameterization of the linear vehicle Bicycle Model was shown to have several advantages over the traditional parameterization. First, the available model data have the appealing form of a Gaussian distribution about a line in the non-dimensional pi-space. This data suggests an 'average' and a 'standard deviation' of vehicle parameters. In addition, this allows vehicle-to-vehicle comparisons and numerically defines a parameter field over which a vehicle controller should be robust.

Second, a duality between velocity and cornering stiffness variation effects on vehicle dynamics has been suggested. The cornering stiffness variation can be cast as a road friction variation. Much work has been conducted in the vehicle controls community on each of these topics separately, and this work suggests perhaps these efforts can be unified in some manner.

Third, the non-dimensionalization approach was used to discover physical relationships inherently present between vehicle parameters. As an example, the well-known oversteer critical velocity was re-cast into the non-dimensional framework. It was demonstrated that the physical relationships between non-dimensional parameters can be captured by simple functional forms such as lines. In the case of vehicles, the pi-space is described fully by a multi-dimensional line with experimental data appearing to have a Gaussian distribution about this line.

Finally, the approach was used to obtain a robust controller where the perturbations were made with respect to non-dimensional parameters. Implementation of this controller was performed both in simulation and on scaled experiments. Within the specified variations of the non-dimensional parameters, closed loop performance characteristics can be specified.

Future work in this research area will likely continue to amass statistical information on published vehicle data with a goal of precisely defining some of the appropriate distributions. Additionally, the extension of the non-

dimensional formulation to larger variations in system parameters will also be investigated.

Acknowledgments

The authors wish to express their sincere gratitude to NSF for providing the opportunity to conduct this research through an NSF Graduate Fellowship. In addition, the authors wish to thank David Lynch for his assistance in conducting vehicle tests.

References

1. Alleyne A. 1997. A Comparison of Alternative Intervention Strategies for Unintended Roadway Departure (URD) Control. *Vehicle System Dynamics* 27:157-186.
2. Brennan S. 1999. Modeling and Control Issues Associated with Scaled Vehicles [Masters]: University of Illinois at Urbana-Champaign. 179 p.
3. Brennan S, Alleyne A. 1999. A Scaled Testbed for Vehicle Control: the IRS. *Proc. of the 1999 IEEE Conference on Control Applications*:327-332.
4. Buckingham E. 1914. On Physically Similar Systems; Illustrations of the use of dimensional equations. *Physical Review* 4:345-376.
5. Gahinet P, Nemirovski A, Laub AJ, Chilali M. 1995. *LMI Control Toolbox - For Use with MATLAB*. Natick, MA: Mathworks.
6. Guldner J, Tan HS, Patwardhan S. 1996. Analysis of Automatic Steering Control for Highway Systems with Look-Down Lateral Reference Systems. *Vehicle System Dynamics* 26:243-269.
7. Horiuchi S, Yuhara N, Takei A. 1996. Two Degree of Freedom H-infinity Controller Synthesis for Active Four Wheel Steering Vehicles. *Vehicle System Dynamics Supplement* 25:275-292.
8. Ono E, Takanami K, Iwama N, Hayashi Y, Hirano Y, Satoh Y. 1994. Vehicle Integrated Control for Steering and Traction Systems by Mu-Synthesis. *Automatica* 30(11):1639-1647.
9. Shiotsuka T, Nagamatsu A, Yoshida K. 1993. Adaptive Control of 4WS System by Using Neural Network. *Vehicle System Dynamics*:411-424.
10. Shladover S. 1995. Review of the State of Development of Advanced Vehicle Control Systems (AVCS). *Vehicle System Dynamics* 24(6-7):551-595.
11. Tagawa Y, Ogata H, Morita K, Nagai M, Mori H. 1996. Robust Active Steering System Taking Account of Nonlinear Dynamics. *Vehicle System Dynamics Supplement* 25:668-681.
12. Wong JY. 1993. *Theory of Ground Vehicles*. New York: J. Wiley & Sons.
13. Zhou K, Doyle J, Glover K. 1996. *Robust and Optimal Control*. Upper Saddle River, NJ: Prentice Hall.